Carbohydrate Polymers 87 (2012) 2291–2298

Contents lists available at SciVerse ScienceDirect

Carbohydrate Polymers

journal homepage: www.elsevier.com/locate/carbpol

Fibrous cellulose nanocomposite scaffolds prepared by partial dissolution for potential use as ligament or tendon substitutes

Aji P. Mathew[a,*], Kristiina Oksman[a], Dorothée Pierron[b], Marie-Françoise Harmand[b]

[a] Wood and Bionanocomposites, Division of Materials Science, Department of Engineering Sciences and Mathematics, Luleå University of Technology, 97187 Luleå, Sweden
[b] Laboratoire d'Evaluation des Matériaux Implantables (LEMI), Technopole Bordeaux-Montesquieu, 2 allée François Magendie, 33650 Martillac, France

ARTICLE INFO

Article history:
Received 5 September 2011
Received in revised form 6 October 2011
Accepted 26 October 2011
Available online 3 November 2011

Keywords:
Cellulose
Composite
In vitro test
Ligament
Tendon
Mechanical properties

ABSTRACT

Fibrous cellulose nanocomposites scaffolds were developed and evaluated for their potential as ligament or tendon substitute. The nanocomposites were prepared by partial dissolution of cellulose nanofiber networks using ionic liquid at 80 °C for different time intervals. Scanning electron microscopy study indicated that partial dissolution resulted in fibrous cellulose nanocomposites where the dissolved cellulose nanofibers formed the matrix phase and the undissolved or partially dissolved nanofibers formed the reinforcing phase. Mechanical properties of the composites in simulated body conditions (37 °C and 95% RH) after sterilization using gamma rays was comparable to those of natural ligaments and tendons. Stress relaxation studies showed stable performance towards cyclic loading and unloading, further confirming the possibility for using these composites as ligament/tendon substitute. *In vitro* biocompatibility showed a positive response concerning adhesion/proliferation and differentiation for both human ligament and endothelial cells. Prototypes based on the cellulose composite were developed in the form of tubules to be used for further studies.

1. Introduction

Cellulose being a natural polymer, insoluble in water and degradable in nature by microbial and fungal enzymes and having limited degradation in animal and human tissues, is a potential raw material for medical implants (Miyamoto, Takahashi, Ito, Inagaki, & Noishiki, 1989). Cellulose based materials like cellulose sponge and cellulose acetate, etc. are found to induce only negligible foreign body and inflammatory responses and are therefore considered as biocompatible (Märtson, Viljanto, Hurme, & Saukko, 1998; Miyamoto et al., 1989). In the recent years bacterial cellulose comprising of nanofibers is being the most widely used form of cellulose in biomedical application owing to its properties like high mechanical properties, biocompatibility, biodegradability, etc. (Bodin, Bäckdahl, Gustafsson, Risberg, & Gatenholm, 2006; Kim, Cai, & Chen, 2010; Märtson et al., 1998; Miyamoto et al., 1989; Ping et al., 2009; Svensson et al., 2005; Zaborowska et al., 2010). Cellulose has also been successfully used as scaffold for tissue engineered meniscus and blood vessels (Bodin et al., 2006; Svensson et al., 2005).

In the human body the main function of the tendons is to transfer the force due to muscle contraction to the bones whereas ligaments stabilize the joints preventing abnormal movements (O'Connor & Zavatsky, 1963). Though natural tendons and ligaments are capable of withstanding high stresses, injuries are common in tendons and ligaments, e.g. rupture of the anterior cruciate ligament (ACL), the primary and most important stabilizer for knee (Fu, Bennet, Latterman, & Ma, 1999). In order to facilitate rapid recovery and rehabilitation, artificial prosthesis to replace or repair natural ligaments and tendons have been explored (Bolton & Bruchman, 1983; Chazal et al., 1985; De Santis et al., 2004; Gissefalt, Edberg, & Flodin, 2002; Jenkins, Forster, Mckibbin, & Ralis, 1977; Legnani, Ventura, Terzaghi, Borgo, & Albisetti, 2010; McCartny, Tolin, Schwenderman, Freidmen, & Woo, 1993; Meyers, Chen, Lin, & Seki, 2008; Migliaresi & Nicolais, 1980; Nachemson & Evans, 1968). However, most of these materials did not possess the same biomechanical properties like the native structure and were known to show irreversible elongation, rupture and formation of wear debris. Experimental and clinical ligament reconstruction studies have generally demonstrated poor long-term results due to persistent pain, sterile effusions, arthritis, and mechanical breakdown of the synthetic polymers (McCartny et al., 1993).

During the 1970s and 80s, various synthetic materials were designed to act as a permanent ligament/tendon replacement device (Bolton & Bruchman, 1983; Jenkins et al., 1977; McCartny et al., 1993). Synthetic polymers clinically evaluated for ACL reconstruction include polytetrafluoroethylene (Gore-Tex), polyethylene terephthalate (Dacron; Stryker-Meadox and

* Corresponding author. Tel.: +46 920493336.
E-mail address: aji.mathew@ltu.se (A.P. Mathew).

0144-8617/$ – see front matter © 2011 Elsevier Ltd. All rights reserved.
doi:10.1016/j.carbpol.2011.10.063

Leeds-Keio ligaments), carbon fibers (Integraft), and braided polypropylene (Kennedy Ligament Augmentation Device) (Bolton & Bruchman, 1983; Jenkins et al., 1977; McCartny et al., 1993). In the recent years several composite materials have been developed and studied with the aim to obtain suitable materials to replace natural ligaments and tendons (Chazal et al., 1985; De Santis et al., 2004; Hukins, Leahy, & Mathias, 1999; Iannace, Sabatini, Ambrosio, & Nicolais, 1995; Meyers et al., 2008; Migliaresi & Nicolais, 1980; Nachemson & Evans, 1968). Artificial tendon made of composites consisting of poly (HEMA) reinforced with polyethylene terephthalate (PET) fibers as well as PET reinforced polyurethane composites for use as ligament prostheses were reported earlier (De Santis et al., 2004; Migliaresi & Nicolais, 1980).

De Santis et al. (2004) studied ligament and tendon substitution with carbon fiber composites and reported a measured maximum strength of 28 MPa and strain of 30% for natural ligament and a maximum strength of 38 MPa and strain of 18%, for tendons. Nachemson and Evans (1968) reported a lower strength value for the human ligament, being only 4.4 ± 3.6 MPa and Chazal et al. (1985) reported for human ligament a strength of 15 ± 5 MPa with a strain of about 20%. This wide variation in mechanical properties indicate that the mechanical behaviour of biological tissues like tendons/ligaments is complex and is influenced by extraction location and method, age of the person, testing conditions of temperature and humidity used, loading rate, shape of the test piece, etc.

In the current study the attempt have been to use wood based cellulose in nanoscale to develop artificial ligaments and tendons with mechanical properties similar or better than natural ligaments or tendons. While developing artificial tendons or ligaments biocompatibility, mechanical properties as well as resistance to *in vivo* moisture, temperature conditions and cyclic loading conditions need to be considered. Since natural tissues function at 37 °C it is advantageous to measure the properties at this temperature, even though elevated temperatures may dehydrate the specimen and affect its properties (Hukins et al., 1999).

Cellulose in nanoscale has been successfully isolated from various plant and animal resources and is of great interest due to its renewable nature, good mechanical properties and large specific surface area (Hubbe, Rojas, Lucia, & Sain, 2008; Oksman, Mathew, & Sain, 2009). The current report is unique because of the use of biobased materials for the development of medical application and is expected to provide superior mechanical properties as well as biocompatibility and non-toxicity as required for biomaterials. The fibrous nanocomposite preparation by partial dissolution has been reported earlier by researchers where micro-sized fibers were used as starting materials (Duchemin, Mathew, & Oksman, 2009; Nishino, Matsuda, & Hirao, 2004). Nanofibers were used in this study considering the possibility to get more homogeneous and uniform product as well as improved fiber matrix interaction and mechanical properties owing to high surface area available for nanocelluloses. The processing and characterisation of the nanocomposites, especially in simulated body conditions of 37 °C and high relative humidity conditions (98%) are included in this work. This study is expected to provide valuable insights on the use of fibrous nanosized cellulose in the development of artificial ligaments and tendons. The developed fibrous cellulose composite is finally fabricated into a prototype.

2. Experimental

2.1. Materials

Special cellulose (Domsjö Fabriker AB, Sweden) from Norway spruce with a cellulose content of >94% was used as starting material for the fibrillation process. Nanofibers were isolated from the special cellulose by mechanical fibrillation method, which is reported elsewhere (Mathew, Stelte, & Oksman, 2009). Fig. 1A shows the fibrous nanocellulose with diameters in the range of 10–40 nm obtained after the mechanical isolation process.

1-Butyl-3-methylimidazolium chloride ($[C_4mim]Cl$) with a purity >95% from BASF (category #38899) was used for the partial dissolution, without further purification.

2.2. Methods

2.2.1. Preparation of fibrous nanocomposites

The fibrous nanocomposites were prepared in two steps, first a low concentration aqueous nanofiber suspension (0.5 wt%) was used to prepare nanofiber networks. This suspension was filtered using a filter press under vacuum until all the water was drained off. The final drying was done by heating at 100 °C between two heated plates for 1 h and then for 6 h at 60 °C at 35 MPa pressure. These nanofiber networks are referred to as NF_0.

The second step was to prepare fibrous nanocomposites. Nanofiber networks were dried thoroughly in a vacuum oven to remove any residual moisture and treated with 15 mL ionic liquid at 80 °C for 90 and 120 min, to prepare fibrous nanocomposites with two degrees of dissolution. The partially dissolved networks were then plunged into water to stop dissolution and to precipitate the dissolved cellulose. After that, the networks were thoroughly washed in excess of water to remove all residual ionic liquid. The excess of water was then wiped off using a paper towel, and dried in a hot press at 60 °C. The prepared fibrous nanocomposites were referred to as NF_{90} and NF_{120} based on time of dissolution.

2.2.2. Prototype development

The cellulose nanofiber networks were prepared and coated with ionic liquid. These coated films were rolled into tubules and kept at 80 °C for 90 min to carry out partial dissolution. After that, partially dissolved tubules were kept immersed in water for 12 h to stop the dissolution and precipitate the dissolved cellulose. The tubes were rinsed in a water bath for 48 h to remove all residual ionic liquids.

2.3. Characterisation

2.3.1. Scanning electron microscopy (SEM)

The morphology of the composites as well as the prototypes was studied using a JEOL JSM 6460 LV, scanning electron microscope. The samples were cryogenically fractured using liquid nitrogen and sputter coated with gold to avoid charging.

2.3.2. X-ray diffraction (XRD)

Crystallinity studies of the composites were done using a Philips X'pert MRD X-ray diffractometer, Philips Electronics N.V. (USA) operated at 40 kV and 45 mA. The samples were exposed for a period of 1.5 s for each angle of incidence (θ) using a Cu Kα X-ray source with a wavelength (λ) of 1.541 Å. The angle of incidence was varied from 5° to 40° at increments of 0.05°. The percentage crystallinity index (C_{Ir}) was measured using the Segal empirical method (Segal, Creely, Martin, & Conrad, 1959):

$$C_{Ir} \quad (\%) = \frac{(I_{200} - I_{am})}{I_{200}} \times 100 \tag{1}$$

where I_{200} is the intensity value for the crystalline cellulose, and I_{am} is the intensity value for the amorphous cellulose.

2.3.3. Water uptake

The samples used for water sorption studies were circular discs, 20 mm in diameter, cut from films conditioned at 5% relative humidity. The cut samples initial weight and dimensions were

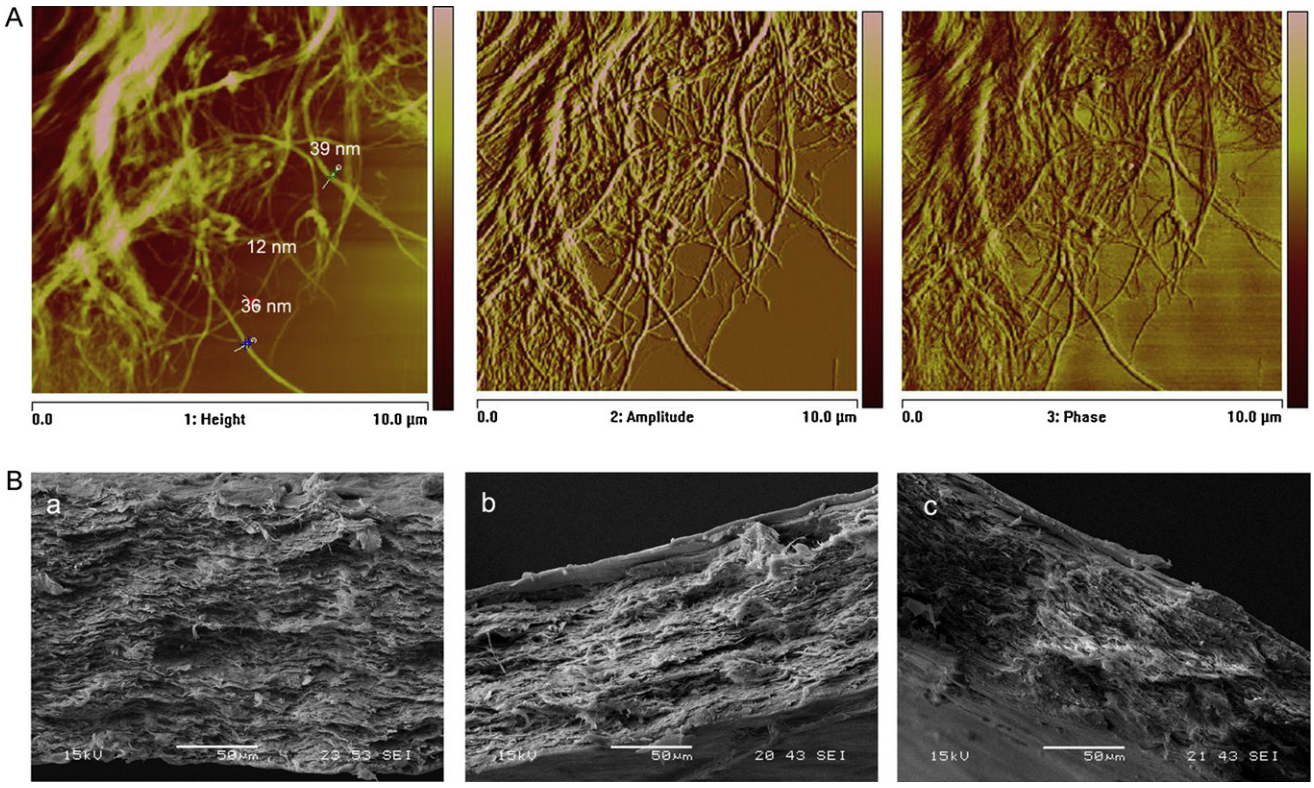

Fig. 1. (A) Atomic force microscopy images of the used cellulose nanofibers; height, amplitude and phase images. (B) Scanning electron microscopy of the (a) undissolved nanofiber network and the nanocomposites with (b) 90, and (c) 120 min of dissolution.

determined. After this, the circular samples were kept immersed in distilled water. The samples were removed at appropriate time intervals, gently blotted with tissue paper to remove excess water on the surface of the films and weighed. This process was continued until equilibrium swelling was reached which was indicated by constant weight. The collected data was used for further calculations and analysis.

2.3.4. Mechanical properties

Tensile properties of the nanofiber network and the fibrous nanocomposites were tested using a Shimadzu Autograph AG-X Universal tester using a strain rate of 5 mm/min and a load cell of 1 kN. The samples were in the form of strips about 6 mm in width and 50 mm in length. Two different testing conditions were used: (a) dry condition at room temperature and (b) wet conditions at 37 °C and 92% RH. The gauge length of 20 mm was used in all cases and the crosshead movement was used to measure the strain. In the case of wet samples, the samples were conditioned at 98% RH and immediately transferred to the testing chamber maintained at 37 °C and 92% RH. Each sample was allowed to equilibrate in the chamber for 5–10 min prior to testing. The data presented is based on at least 8 samples. Some of the selected samples were tested using the same procedure after sterilization using gamma rays.

Short-term stress relaxation of the materials was studied at 37 °C, using a dynamic mechanical analyser (DMA 800, TA Instruments). The stress was applied for 30 min, followed by 10 min of relaxation and tested for 4 cycles. The strain was kept constant at 0.5%.

2.3.5. Cytocompatibility studies

Cytotoxicity was performed in direct contact and using a liquid extract according to the ISO standard procedure (ISO 10993-5: 2009) "Biological evaluation of medical devices – Part 5: Test for *in vitro* cytotoxicity". The liquid extract was performed according to ISO 10993-12: 2007 (ISO 10993-12: 2007): "Biological evaluation of medical devices – Part 12: Sample preparation and reference materials" (extraction vehicle: culture medium, ratio: 3 cm^2/mL – incubation time 24 h – gentle agitation: 8 rockings/min). The cell system used was Balb/c 3T3 (ATCC CCL 163) checked free from mycoplasma. Positive (BSI disc from Portex Ltd., or phenol at 0.64 mg/mL) and negative (Termanox disc, or culture medium) controls were run in parallel.

Culture of human cells: Human ligament explants were obtained from orthopaedic surgery from consenting patients (20–40 years). Human ligament cells (HLC) arising from out-growths were grown in Iscove's Modified Dulbecco's Medium (IMDM, Gibco), supplemented with 10% (v/v) Fetal Calf Serum (FCS) (Gibco). HLC were used at the 6th passage. Human vascular endothelial cells (HEC) arising from human umbilical cord vein according to Jaffe, Nachman, Becker, and Minick (1973) were grown in Iscove's Modified Dulbecco's Medium (IMDM, Gibco), supplemented with 20% (v/v) Fetal Calf Serum (FCS) and 0.4% of ECGS/H (endothelial cell growth supplement/heparin) (Promocell). HEC were used at the 9th passage.

For both cell attachment/proliferation and cell differentiation study, first samples were covered up with complete culture medium and incubated at 37 °C during 3 × 30 min. Precoating with serum proteins mimics "*in vivo*" situation following implantation (adsorbed protein layer).

2.3.6. Cell attachment and proliferation

1 cm^2 samples were placed on the bottom of the wells of a 24-well plate, HLC or HEC were seeded at the starting density of 10×10^3 cells/cm^2. To access cell attachment, adhesion and proliferation on the samples, two approaches were used: Live/Dead staining was performed at 1 and 3 days using a commercially available kit [(Live/Dead viability)/cytotoxicity kit; Molecular Probes, In Vitrogen]. Cells were incubated in the presence of 2 μM calcein AM

Table 1
Sequencing of the used primers for cell differentiation study.

Target genes	Primers sequences[a]	Annealing temp. (°C)	Product leng. (bp)
β-Actin	5′-AGT CCT GTG GCA TCC ACG AAA-3′ 5′-GGA GCA ATG ATC TTG ATC TTC-3′	57	186
Collagen type I (HLC)	5′-CGT GAC CAA AAA CCA AAA GTG C-3′ 5′-GGG GTG GAG AAA GGA ACA GAA A-3′	54	186
Collagen type III (HLC)	5′-CCC ACT ATT ATT TTG GCA CAA CAG-3′ 5′-GCA TGG TTC TGG CTT CCA GA-3′	48	99
Integrin αV (HLC)	5′-AAA GCG AAC ACG ACC CAG C-3′ 5′-GCC GTC ACC ATT GAA GTC TCC-3′	57.2	582
Integrin β3 (HLC)	5′-CAG AGG AAG GGA CAC CAA GC-3′ 5′-TCA CAA GGC AGC CAA GAG G-3′ 5′-CGG GAC ACC TAC TCT CAT ACT-3′	54.2	673
CD31 (HEC)	5′-CCT GCT GAC CCT TCT GCT CTG-3′ 5′-TAC AGT CGT GGT GGA GAG TGC-3′	65	74

[a] A T C G represent the standard nucleotides that generate bases used especially for designing PCR primers, where A, adenine; G, guanine; C, cytosine; T, thymine. Nucleotides are molecules that when joined together make up the structural units of DNA.

and 4 μM ethidium homodimer solution for 20 min, at 37 °C in the dark. Cytoplasm of live cells fluoresces due to DNA binding of ethidium homodimer in cells compromised nuclear membranes. The second approach is a quantitative method; at the end of each incubation period, cells were detached by trypsinization and counted using hemacytometer.

2.3.7. Cell differentiation

Cell differentiation was performed using 1 and 3 days incubation periods. Cells were seeded onto the test material at 100×10^3 cells/cm^2. Total RNA was extracted from HLC or HEC using the RNeasy Micro kit (Qiagen). cDNA was synthesized from 1 ng total RNA using Verso TM cDNA Synthesis kit (Thermo Scientific). PCR (TC 3000G; Techne) was performed to analyze genes related to HLC (Collagen type I and III, Integrin αv, Integrin β3) and to HEC (CD31). Housekeeping gene (β-actin) was analyzed in parallel. Sequences of the used primers are described in Table 1.

3. Results and discussion

3.1. Structure of the nanofiber network and the fibrous nanocomposites

The morphology of the fibrous nanocomposites is an important parameter, which determines the mechanical performance of the material. The SEM images of the nanofiber networks and the fibrous nanocomposites obtained after 90 and 120 min of dissolution are given in Fig. 1B. The NF0 shows cellulose nanofibers arranged in a layered structure. In the micrographs of NF90 and NF120 (1Bb and 1Bc) also cellulose nanofibers are visible indicating that only partial dissolution has occurred. It was found that in both these materials the cellulose dissolution was mostly on the surface and limited dissolution of nanofibrils has occurred in the bulk resulting in skin–core morphology. NF90 and NF120 can be considered as consolidated nanocomposites where the dissolved cellulose forms the matrix phase and the undissolved cellulose nanofibers forms the reinforcing phase.

The crystallinity data of the nanofiber networks before and after dissolution are given in Fig. 2. The diffraction peaks at $2\theta = 14.2°$, 16° and 22.3° showed that the cellulose I structure was retained after the partial dissolution using ionic liquids and that the crystallinity was not significantly affected by the dissolution process. However the percentage crystallinity decreased from 73% for the undissolved networks to 63–65% partially dissolved networks.

3.2. Water susceptibility of the nanofiber network and the fibrous nanocomposites

For use of the developed materials as implants it is important to know the water uptake capability as well as their change in dimensions while inside the body. Water uptake of the developed materials was studied in order to understand the sorption behaviour in humid conditions and the sorption curves are shown in Fig. 3. It was found that the uptake was highest for the nanofiber networks and decreased after partial dissolution. The uptake is about 104% for the nanofiber networks, which was reduced to 87% and 95% for NF_{90} and NF_{120}, respectively. This can be explained by the higher porosity in the nanofiber networks compared to the partially dissolved fibrous nanocomposites. In the partially dissolved nanocomposites, the dissolved cellulose fraction acts as a matrix and fills the pores between the nanofiber networks forming a consolidated structure. Additionally the nanofibers remaining in the consolidated structure have the potential to reduce the water uptake by restricting the mobility of the matrix phase. It was noted

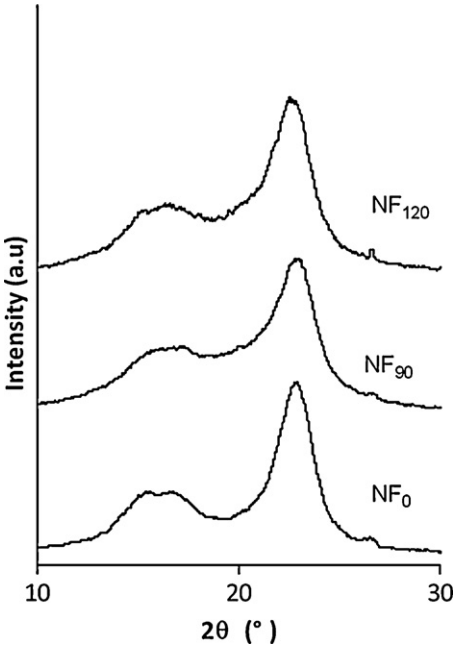

Fig. 2. WAXD patterns of undissolved nanofiber network and the fibrous nanocomposites obtained by partial dissolution.

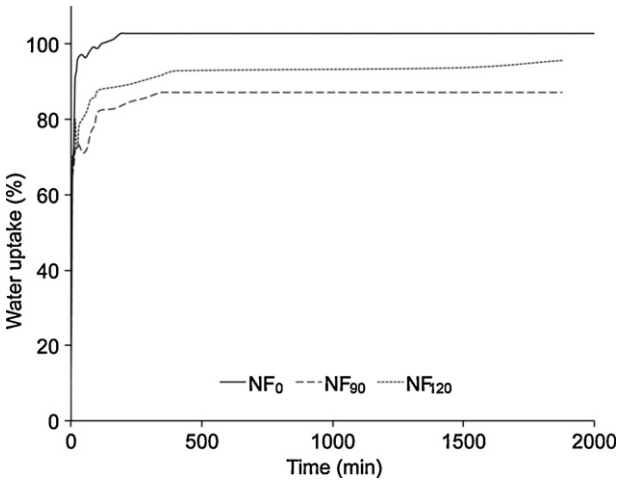

Fig. 3. Water sorption behaviour of the undissolved nanofiber network and the fibrous nanocomposites obtained by partial dissolution.

that the NF_{90} samples showed the lowest water uptake indicating possibly a good consolidation as well as restriction in matrix mobility. Water content in natural ligaments and tendons is reported to be 60% or above (O'Connor & Zavatsky, 1963) and the current materials show higher water retention.

Another interesting observation from the study was that the uptake was instantaneous and high during the first few minutes and did not increase substantially after that. It was also noticed that the size of the samples were changed only by about 5–10% (image not shown) after water exposure suggesting that these materials have good dimensional stability in humid conditions. This is considered advantageous due to limited changes in moisture uptake and the dimensions, especially if moisture is equilibrated (preconditioned) before implanting these materials in the body.

3.3. Mechanical properties

Mechanical properties of the developed materials were tested in room conditions as well as in simulated body conditions to evaluate its potential as ligament/tendon substitutes. In this study we aimed to obtain a maximum strength of in the range of 28–38 MPa and strain of 18–30% based on the measured values of mechanical properties of natural ligament or tendon, reported by De Santis et al. (2004). The data from tensile testing (room and simulated body conditions) are given in Table 2. The results show that the nanofiber networks have strength of 105 MPa and modulus of 6.6 GPa. These values are much higher than the requirement for tendons and ligaments (De Santis et al., 2004). The tensile strength and modulus showed a tendency to increase after partial dissolution. However the strain at break was only about 7–13% and was lower than the requirement. In the case of simulated body conditions, the strength and modulus decreased drastically for the nanocomposites where as the strain increased, compared to the corresponding dried materials (see Table 2). It was also found that the effect of moisture and temperature was higher on the partially dissolved composites compared to the nanofiber networks. It was however noted that the values of strength and strain of the studied materials are in the required range for ligament and tendons indicating that all the developed materials have the potential to be used as ligament or tendon.

Table 2
Tensile properties of cellulose nanofiber networks and the fibrous cellulose nanocomposites in room conditions and in simulated body conditions (98% RH and 37 °C).

Sample	Tensile strength (MPa)	Strain (%)	*E*-Modulus (GPa)
NF_0	105.9 ± 5.5	10.3 ± 0.6	6.6 ± 0.5
NF_{90}	112.2 ± 6.5	7.4 ± 0.8	8.2 ± 0.8
NF_{120}	117.9 ± 6.6	12.8 ± 1.4	6.8 ± 0.6
NF_0 (wet, 37 °C)	64.5 ± 4.9	23.4 ± 2.1	0.50 ± 0.14
NF_{90} (wet, 37 °C)	36.2 ± 3.3	21.3 ± 3.8	0.35 ± 0.08
NF_{120} (wet, 37 °C)	37.4 ± 2.8	20.0 ± 3.1	0.32 ± 0.11

Table 3
Tensile properties of cellulose nanofiber networks and the fibrous cellulose nanocomposites after sterilization using gamma rays in simulated body conditions (98% RH and 37 °C).

Sample	Tensile strength (MPa)	Strain (%)
NF_{90}, dry, sterilized	90.1 ± 4.2	14.3 ± 0.8
NF_0 (wet, 37 °C), sterilized	25.1 ± 1.4	20.1 ± 1.6
NF_{90} (wet, 37 °C), sterilized	29.1 ± 1.7	27.7 ± 4.4

In order to further confirm the suitability of these materials in biomedical application, these materials were tested after sterilization using gamma radiations. The results of the tensile testing are given in Table 3. It was found that sterilization, the material properties were lower in both, room and simulated body conditions compared to the corresponding non-sterilized ones. However, it may be noted that the properties of these materials are still within the acceptable range for use in ligament or tendon application. Fig. 4

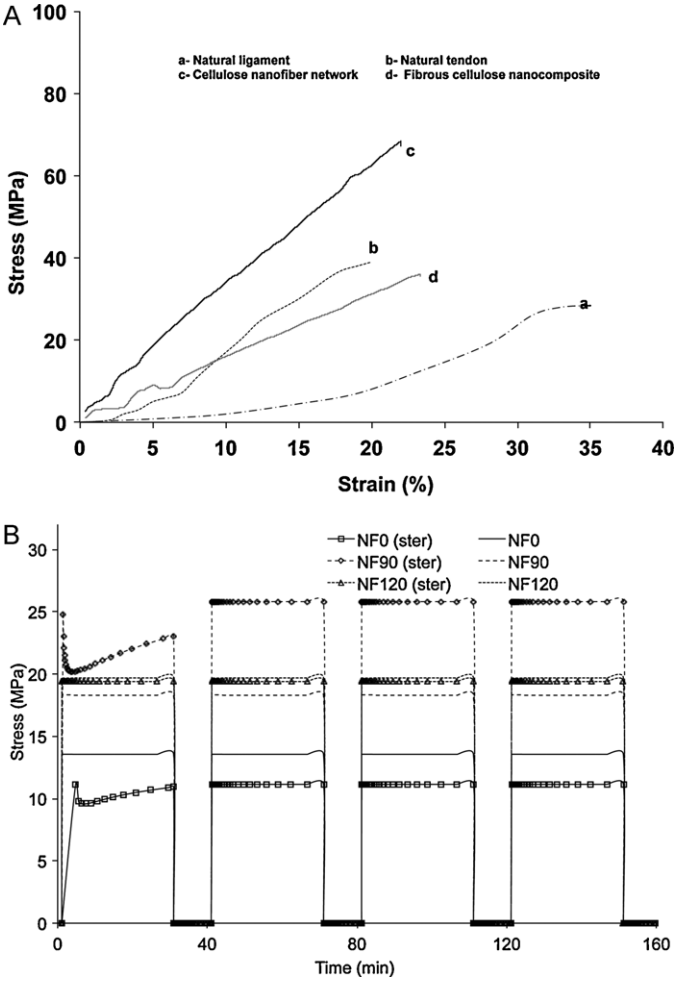

Fig. 4. (A) Comparison of the stress–strain behaviour of sterilized cellulose nanofiber network and the fibrous nanocomposites with that of natural ligament and tendon. (B) Stress relaxation behaviour of nanofiber network and the nanocomposites at 37 °C before and after sterilization, measured using dynamic mechanical thermal analyser.

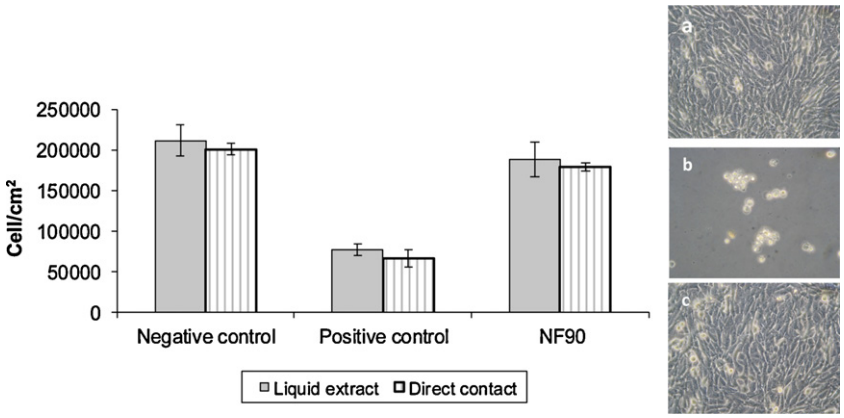

Fig. 5. Cytotoxicity study in direct contact and using a liquid extract (ISO 10993-5). Iconographies of direct contact (320×): (a) negative control, (b) positive control, and (c) NF_{90}.

shows the comparison of the stress–strain curves of the nanofiber networks and fibrous nanocomposites (NF_{90}) after sterilization in comparison with that of natural ligament and tendon. The mechanical performance of natural ligament and tendons is very complex and usually shows two distinct regions: the first one (known as toe region) due to the matrix phase and the second one due to the response of the fibers when they are aligned in the loading direction (De Santis et al., 2004). Even though the stress–strain responses are not exactly the same, a very similar behaviour with a 'toe like region' at the beginning and the second phenomenon due to disentangling and orientation of the nanofibers under stress is visible from the stress–strain curves of the nanofiber networks as well as the nanocomposites, especially in the sterilized ones. The stress–strain curves also showed that the deformation of the nanofiber networks and the fibrous nanocomposite is elastic in nature and no yielding or plastic deformation was observed which is a favourable factor to utilize these materials for the development of ligament or tendon.

Further studies on the mechanical stability of the developed materials were carried out by short-term stress relaxation, where the samples are subjected to cyclic loading and unloading, with a constant strain of 0.5%. The data from the stress relaxation test at 37 °C before and after sterilization is given in Fig. 4. In the case of un-sterilized samples, the fibrous nanocomposite showed higher stress than the undissolved nanofiber networks and all the materials showed very stable performance under cyclic stress. In this case NF_{120} showed the highest stress values. However after the sterilization process it was found that the stress values decreased for the nanofiber networks where as it increased for NF_{90} samples. The sterilization did not have any significant effect on the NF_{120} samples. During stress relaxation test it was also noticed that the materials showed higher stress after the first cycle, which was probably due to dis-entangling and orientation of the nanofibers under load. This phenomenon was not observed after the first cycle and the maximum stress remained constant in the subsequent cycles.

The mechanical property studies indicated better mechanical performance for NF_{90}, which may be due to an optimal dissolution, which leads to the composites with best fiber/matrix ratio as well as favourable interactions. Therefore NF_{90} samples were considered as the potential candidate for ligament/tendon application.

3.4. Cytocompatibility

3.4.1. Cytotoxicity

The results of cytotoxicity test are presented in Fig. 5. The negative and positive controls validate the test system (cell balb3T3) and the assay. A slight cytostatic effect (≈8%) was noticed for the fibrous nanocomposite, NF_{90}, obtained by treating the nanofiber network with ionic liquid, compared to the negative control. However, no cytotoxic effect was found biologically significant because for both liquid extract and direct contact method, cell viability (cell/cm^2) after 24 h of contact between cell and test material, is greater than

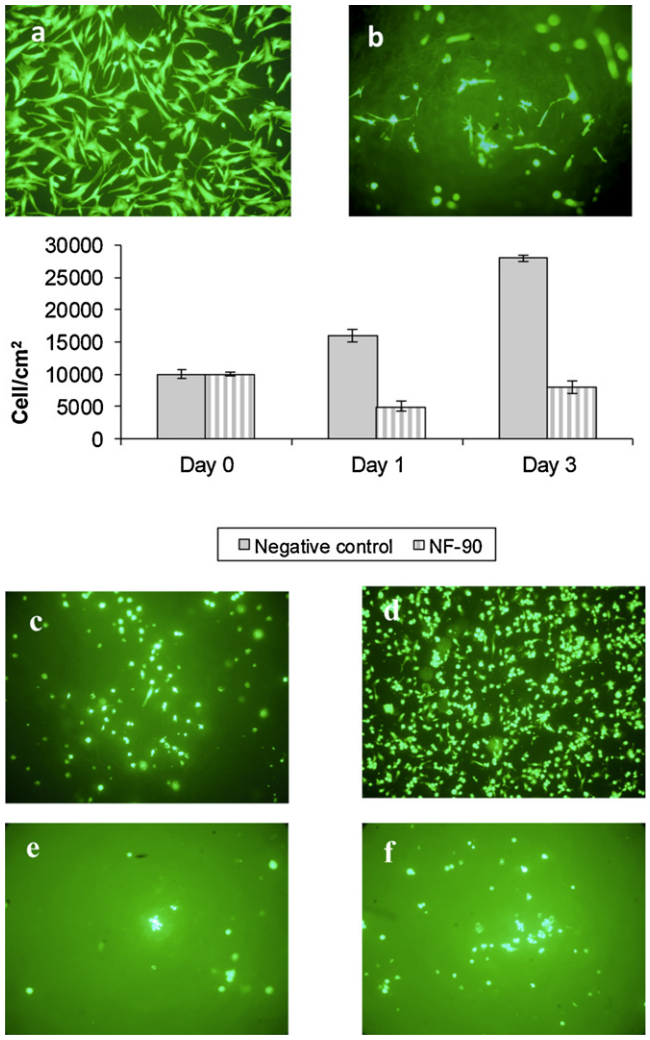

Fig. 6. HLC and HEC adhesion (Live/Dead test) and proliferation. (A) HLC adhesion (day 1) – Iconographies of proliferation study (100×): (a) HLC-negative control-day 1, (b) HLC-NF_{90}-day 1; (B) HLC proliferation (day 1 and day 3); (C) HEC adhesion (Live/Dead test) (days 1 and 3) – Iconographies of proliferation study (100×): (c) HEC-negative control-day 1; (d) HEC-negative-control-day 3; (e) HEC-NF_{90}-day 1; (f) HEC-NF_{90}-day3.

70%, according to ISO 10993-5, indicating that test material NF_{90} is non-cytotoxic (see the graph on the left).

The iconographies on the right show the cells on the controls or test material after 24 h of direct contact. Fig. 5a shows a monolayer of established cell line (Balb/c 3T3) after 24 h of contact with thermanox disk (negative control) where as Fig. 5b shows that cells no cell layer are present after contact with BSI (positive control). In the case of positive control the cells were found to be detached and dead.

In Fig. 5c one can observe a nice cell monolayer on NF_{90}, similar to negative control with cells morphology comparable to negative control. This confirmed the non-cytotoxicity of NF_{90} samples.

3.4.2. Cell adhesion and proliferation

Fig. 6A (a and b) shows HLC adhesion at day 1 on negative control (polystyrene of the culture wells) and on NF_{90}. HLC adhere on NF_{90} with a round shape (60%) or spindle-like morphology, whereas on negative control the spindle-like morphology is highly dominant. At day 1 (Fig. 6B) HLC adhesion on NF_{90} is 50% of initial seeding, whereas on the negative control all cells adhered and start to proliferate (160% of initial seeding). Thereafter at day 3 HLC proliferated slowly (+38% *versus* day 1) on NF_{90} and more rapidly on negative control, which was expected (+75% *versus* day 1). Doubling time of HLC is 2 days on plastic and 5 days on NF_{90}. Fig. 6C (a–d) shows HEC adhesion after 1 day and 3 days of incubation on NF90 and negative control. Despite auto-fluorescence of NF_{90} one can observe a very low cell adhesion at day 1 (Fig. 6C (c)) followed by cell proliferation shown at day 3 (Fig. 6C (d)). Obviously negative control colonization is much more better (Fig. 6C (a and b)).

This preliminary study has shown that NF_{90} is able to support HLC and HEC adhesion and proliferation.

3.4.3. Phenotype expression

Expression of mRNA of interest was investigated at day 1 and day 3. Results are shown in Fig. 7A and B. The housekeeping gene (endocontrol) was nicely expressed on both control and NF_{90}, for both culture systems, HLC and HEC.

mRNA expression of collagen type I, a typical marker of HLC, and collagen type III, on early synthesized collagen in ligament healing were detected and measured for both control (validation of the test system) and NF_{90}. Moreover integrin submit α_v and integrin submit β_3 mRNA (not shown) was found (to be expressed) on both substrates. These plasma membrane receptors indicate adhesion of cells either on extracellular matrix components or on material substrates. The fact that these genes are expressed confirms the results of HLC adhesion on NF_{90} and seems to suggest the formation of focal adhesion points.

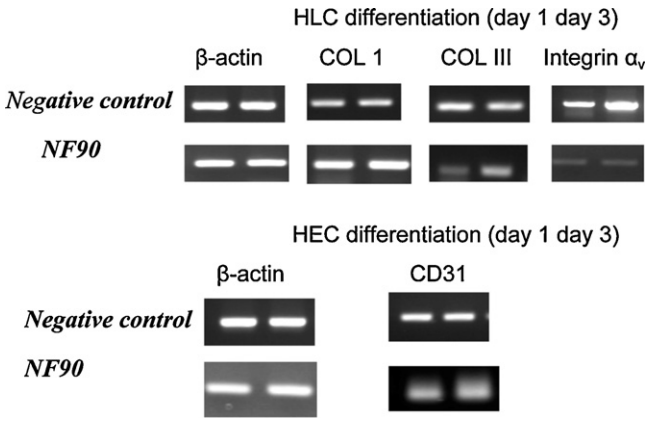

Fig. 7. HLC and HEC mRNA expression at day 1 and day 3.

Concerning HEC behaviour, CD31mRNA, a cell surface marker typical of vascular endothelial cells, implicated in junctions between neighbouring cells, was nicely expressed on both control (validation of the test system) and NF_{90}. This result suggests that NF_{90} should allow endothelial adhesion and growth, and in situ angiogenesis to provide essential nutriment diffusion for HLC phenotype expression, especially collagen synthesis.

3.5. Prototypes

The photograph as well as the micrographs of the prototypes is shown in Fig. 8. The photograph shows tube shaped ligament substitutes made up of nanofibers treated with ionic liquid for 90 min at 80 °C, in phosphate buffer medium (PBS). The prototypes were stable in PBS medium and maintained their structural and dimensional stability. The cross-section of the prototype was examined using SEM to understand the microstructure of the prototype. It was found that the prototype consists of layers of partially dissolved cellulose nanofibers arranged in concentric circles with limited adhesion between the layers (Fig. 8b). The detailed view of the single layer showed the nanofibers embedded in the dissolved cellulose matrix.

Based on the studies of mechanical properties and the biocompatibility on NF_{90} materials, it is expected that the developed prototype will have excellent mechanical properties and stability in body conditions and at the same time is non-toxic and biocompatible. Further, *in vivo* biomechanical tests on the prototypes to evaluate its suitability as ligament/tendon substitute are under progress and will be reported subsequently.

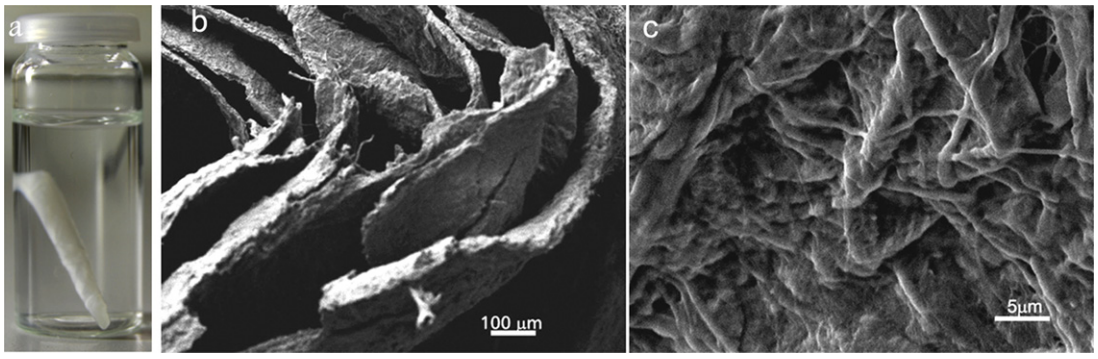

Fig. 8. Photograph of (a) tubular prototypes in PBS medium and the microstructure of the prototypes (b) overview (c) detailed view.

4. Conclusions

Cellulose nanofibers based fibrous composites were prepared by partial dissolution using ionic liquids and evaluated for its potential as artificial ligaments and tendons.

The morphology studies of the fibrous nanocomposites showed nanofibers embedded in the dissolved cellulose matrix and skin–core morphology with more dissolution on the surface. The studied materials showed good dimensional stability and the water uptake occurred mostly during the first few minutes. The NF_{90}, fibrous nanocomposites, showed the best water resistance in moist conditions.

The mechanical properties of the nanofiber networks and the fibrous nanocomposites before and after sterilization were studied in dry and wet conditions. The sterilized samples showed strength in the range of 25–30 MPa and strain of 20–28%, which is in the required range for tendon or ligament application.

For ligament tissue engineering the interaction of ligament derived-fibroblasts (HLC) with the chosen substrate is fundamental. Cellulose nanofibers, based fibrous nanocomposite, NF_{90}, showed no cytotoxicity, was able to support both HLC and HEC adhesion and growth, together with good cell phenotype expression. These results demonstrate the excellent cytocompatibility of NF_{90}, which seems to be a good candidate to support ligament repair, through angiogenesis and collagen synthesis. Based on the initial results cylindrical prototypes were prepared based on partially dissolved cellulose nanofiber networks and were used for further evaluation. This study indicated that controlled partial dissolution of nanofiber networks will be a viable route to develop biomaterials with good mechanical properties and cytocompatibility required for medical applications.

Acknowledgements

The authors gratefully acknowledge the European Commission for the financial support under the Contract Number NMP4-CT-2006-033277 TEM-PLANT. FINCERAMICA, Italy is acknowledged for sterilization of the samples for characterisations.

References

Bodin, A., Bäckdahl, H., Gustafsson, L., Risberg, B. & Gatenholm, P. (2006). Manufacturing and characterisation bacterial cellulose tubes using two different fermentation techniques. In A. Mendez-Vilas (Ed.), *Modern multidisciplinary applied microbiology: Exploiting microbes and their interactions* (pp. 619–622). Weinheim, Germany: Weinheim, Wiley VC Verlag GmbH & Co. KGaA.

Bolton, C. W. & Bruchman, B. (1983). Mechanical and biological properties of the GORE-TEX expanded polytetrafluoroethylene (PTFE) prosthetic ligament. *Aktuelle Probleme in Chirurgie und Orthopadie*, *16*, 40–51.

Chazal, J., Tanguy, A., Bourges, M., Gaurel, G., Escande, G., Guillot, M., et al. (1985). Biomechanical properties of spinal ligaments and histological study of the supraspinal ligament in traction. *Journal of Biomechanics*, *18*, 167–179.

De Santis, R., Sarracino, F., Mollica, F., Netti, P. A., Ambrosio, L. & Nicolais, L. (2004). Continuous fiber reinforced polymers as connective tissue replacement. *Composites Science and Technology*, *64*, 861–871.

Duchemin, B., Mathew, A. P. & Oksman, K. (2009). All-cellulose composites by partial dissolution in the ionic liquid 1-butyl-3-methylimidazolium chloride. *Composites Part A: Applied Science and Manufacturing*, *40*(12), 2031–2037.

Fu, F., Bennet, C. H., Latterman, C. & Ma, C. (1999). Current trends in ACL ligament reconstruction. *American Journal of Sports Medicine*, *27*, 821–830.

Gissefalt, K., Edberg, B. & Flodin, P. (2002). Synthesis and properties of degradable poly(urethane urea)s to be used for ligament reconstructions. *Biomacromolecules*, *3*, 951–958.

Hubbe, M. A., Rojas, O. J., Lucia, L. A. & Sain, M. (2008). Cellulosic nanocomposites: A review. *Bioresources*, *3*(3), 929–980.

Hukins, D. W. L., Leahy, J. C. & Mathias, K. J. (1999). Biomaterials: Defining the mechanical properties of natural tissues and selection of replacement materials. *Journal of Materials Chemistry*, *9*, 629–636.

Iannace, S., Sabatini, G., Ambrosio, L. & Nicolais, L. (1995). Mechanical behaviour of composite artificial ligaments and tendons. *Biomaterials*, *16*, 675–680.

ISO 10993-12: 2007. Biological evaluation of medical devices – Part 12: Sample preparation and reference materials.

ISO 10993-5: 2009. Biological evaluation of medical devices – Part 5: Test for *in vitro* cytotoxicity.

Jaffe, E. A., Nachman, R. L., Becker, C. G. & Minick, C. R. (1973). Culture of human endothelial cell derived from umbilical veins. Identification by morphologic and immunologic criteria. *Journal of Clinical Investigation*, *52*(11), 2745–2756.

Jenkins, D. H. R., Forster, I. W., Mckibbin, B. & Ralis, Z. A. (1977). Induction of tendon and ligament formation by carbon implants. *Journal of Bone and Joint Surgery*, *59B*, 53–57.

Kim, J., Cai, Z. & Chen, Y. (2010). Biocompatible bacterial cellulose composites for biomedical application. *Journal of Nanotechnology in Engineering and Medicine*, *1*, 011006–110013.

Legnani, C., Ventura, A., Terzaghi, C., Borgo, E. & Albisetti, W. (2010). Anterior cruciate ligament reconstruction with synthetic grafts. A review of literature. *International Orthopaedics (SICOT)*, *34*, 465–471.

Märtson, M., Viljanto, J., Hurme, T. & Saukko, P. (1998). Biocomptibility of cellulose sponge with bone. *European Surgical Research*, *30*, 426–432.

Mathew, A. P., Stelte, W. & Oksman, K. (2009). Mechanical isolation of nanofibers and their utilization in novel nanocomposites for medical applications. In *10th international conference of wood & biofiber plastic composites* Madison, WI, USA, 11–12 May, (pp. 97–103).

McCartny, D. M., Tolin, B. S., Schwenderman, A., Freidmen, M. J. & Woo, S. L. Y. (1993). Prosthetic replacement for anterior cruciate ligament. In D. W. Jackson (Ed.), *The anterior cruciate ligament: Current and future concepts* (pp. 343–356). New York: Raven Press Ltd.

Meyers, M. A., Chen, P.-Y., Lin, Y.-M. A. & Seki, Y. (2008). Biological materials: Structure and mechanical properties. *Progress in Materials Science*, *53*, 1–206.

Migliaresi, C. & Nicolais, L. (1980). Composite materials for biomedical applications. *International Journal of Artificial Organs*, *3*, 114–118.

Miyamoto, T., Takahashi, S., Ito, H., Inagaki, H. & Noishiki, Y. (1989). Tissue biocompatibility of cellulose and its derivatives. *Journal of Biomedical Materials Research*, *23*, 125–133.

Nachemson, A. & Evans, J. (1968). Some mechanical properties of the third human lumbar interlaminar ligament (ligamentum flavum). *Journal of Biomechanics*, *1*, 211–220.

Nishino, T., Matsuda, I. & Hirao, K. (2004). All-cellulose composites. *Macromolecules*, *37*(20), 7683–7687.

O'Connor, J. J. & Zavatsky, A. (1963). ACL forces in activity. In D. W. Jackson (Ed.), *The anterior cruciate ligament* (pp. 5–22). New York: Raven Press.

Oksman, K., Mathew, A. P. & Sain, M. (2009). Novel bionanocomposites: Processing, properties and potential applications. *Plastics, Rubbers and Composites*, *38*(9–10), 396–405.

Ping, W., Yi, S., Yuanyuan, J., Jingtong, Z., Zongliang, W., Yanyan, C., et al. (2009). Study on the feasibility of bacterial cellulose as tissue engineering scaffold. *Advanced Materials Research*, *79–82*, 147–150.

Segal, L., Creely, L., Martin, A. E. & Conrad, C. M. (1959). An empirical method for estimating the degree of crystallinity of native cellulose using X-ray diffractometer. *Textile Research Journal*, *29*, 786–794.

Svensson, A., Niclasson, E., Harrah, T., Panilaitis, B., Kaplan, D., Brittber, M., et al. (2005). Bacterial cellulose as a potential scaffold for tissue engineering of cartilage. *Biomaterials*, *26*, 419–431.

Zaborowska, M., Bodin, A., Bäckdahl, H., Popp, J., Goldstein, A. & Gatenholm, P. (2010). Microporous bacterial cellulose for bone regeneration. *Acta Biomaterialia*, *6*, 2540–2547.